Baroclinic wave packets in an extended quasigeostrophic two-layer model

Wenchang Yang,[1] Ji Nie,[1] Pu Lin,[1] and Benkui Tan[1]

Received 13 December 2006; revised 26 January 2007; accepted 5 February 2007; published 15 March 2007.

[1] An extended quasigeostrophic two-layer model including nonlinear Ekman pumping and nonlinear interface perturbation is used to numerically study the formation and maintenance of baroclinic wave packets. With an initial zonal jet flow of north–south symmetry and small random initial perturbations wave packets of finite amplitude are produced and maintained with an equilibrated wave packet-zonal flow system exhibiting simultaneously downstream-upstream asymmetry and north–south asymmetry, the later of which has not been observed in the past simple quasigeostrophic two-layer modeling studies. The northern upstream part of the wave packets is stronger than its southern upstream counterpart and therefore the peak of time-and-zonal-average eddy kinetic energy associated with the wave packets is shifted poleward while the peak of the time-mean zonal jet flow is shifted equatorward, which is in agreement with the observations.
Citation: Yang, W., J. Nie, P. Lin, and B. Tan (2007), Baroclinic wave packets in an extended quasigeostrophic two-layer model, *Geophys. Res. Lett.*, *34*, L05822, doi:10.1029/2006GL029077.

1. Introduction

[2] In recent years, studies on baroclinic wave packets and storm tracks have been attracted much attention. Observational studies show that baroclinic waves in mid-latitude storm tracks of both the northern Hemisphere and the southern Hemisphere tend to be organized into localized coherent wave packets that clearly exhibit downstream development with the group velocity significantly exceeding the phase speed [*Chang*, 1993; *Berbery and Vera*, 1996; *Chang and Yu*, 1999]. To understand the dynamics of these wave packets is still a big challenge to meteorologists. For localized perturbations in a baroclinic unstable flow, the linear theory predicts an ever expanding of wave packets toward both downstream and upstream which obviously contradicts the observational facts that the downstream development dominates the evolution of the wave packets. No doubt that the nonlinearity somehow plays an important role in the wave packet dynamics. Nonlinear numerical modeling studies show that downstream developing wave packets can be easily observed in either the primitive equations or a simple quasigeostrophic two-layer model [*Simmons and Hoskins*, 1979; *Chang and Orlanski*, 1993; *Lee and Held*, 1993; *Swanson and Pierrehumbert*, 1994; *Esler and Haynes*, 1999] and two possible mechanisms for their maintenance have been suggested though these mechanisms need further observational supports [*Chang*, 2001].

[3] This paper, however, concerns another significant characteristic of the baroclinic wave packets/storm track dynamics: the north–south asymmetry. It has long been known that in both northern and southern Hemispheres the storm tracks and their associated jets do not coincide completely with the peak of storm tracks shifted poleward. Figure 1 shows the statistics of latitudinal distribution of the time-and-zonal-average zonal flow and eddy kinetic energy associated with the baroclinic wave packets for 24 Northern and Southern winters. We see that the peak of the eddy kinetic energy and the peak of the zonal flow are separated with each other with the former shifted to polar side and about 10 degrees of latitude apart. Up to present the dynamics of the north–south asymmetry has been received little attention and will be investigated here in our present paper.

2. The Model and the Numerical Scheme

[4] The model used is two-layer model. The fluid consists of two layers of uniform but distinct densities with light fluid on top, rotating with local angular speed $\Omega \sin \varphi$ about the vertical axis(Ω is the angular speed of rotation of the earth, φ is latitude). The fluid is contained in a channel of width L_y. On a beta-plane a quasi-geostrophic vorticity equation with the divergence-vorticity term retained can be written as

$$\frac{\partial \varsigma_{gi}}{\partial t} + \vec{V}_{gi} \cdot \nabla \varsigma_{gi} + \beta v_{gi} = -\left(f_0 + \varsigma_{gi}\right)\left(\frac{\partial u_i}{\partial_x} + \frac{\partial v_i}{\partial y}\right) = \left(f_0 + \varsigma_{gi}\right)\frac{\partial w_i}{\partial z} \quad (1)$$

where i = 1, 2 correspond to the upper and lower layers, respectively, u_{gi}, v_{gi} are the geostrophic winds and $\varsigma_{gi} = \frac{\partial v_{gi}}{\partial x} - \frac{\partial u_{gi}}{\partial y}$ the geostrophic vorticity. The term $\varsigma_{gi}\left(\frac{\partial u_i}{\partial x} + \frac{\partial v_i}{\partial y}\right)$ is the so-called divergence-vorticity term and was usually omitted in the past studies for one usually thought that the relative vorticity ς_{gi} was small compared with the planetary vorticity f_0. We argue that for the baroclinic wave packets associated with the jet, the divergence-vorticity term $(f_0 + \varsigma_{gi})\left(\frac{\partial u_i}{\partial x} + \frac{\partial v_i}{\partial y}\right)$ as a whole may be significantly different in value in regions of cyclonic vorticity versus anticyclonic vorticity such as in the northern and southern parts of the jet. This is because that the relative vorticity is of opposite signs and the absolute

[1]Laboratory of Severe Storm and Flood Disaster, Department of Atmospheric Sciences, School of Physics, Peking University, Beijing, China.

0094-8276/07/2006GL029077

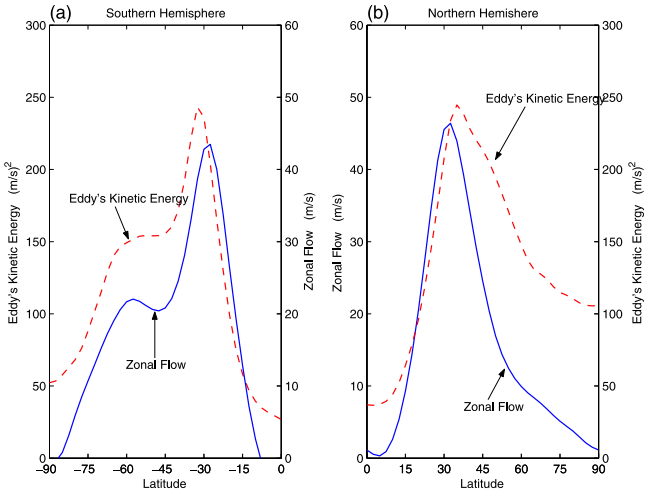

Figure 1. Latitudinal distributions of the time-and-zonal-average zonal flow and eddy kinetic energy on 250 hPa for (a) 24 Southern Hemisphere winters and (b) 24 Northern Hemisphere winters from 1978–1979 winter to 2001–2002 winter. Solid line is the zonal flow and dashed line is the eddy kinetic energy. The data used is the NCEP/NCAR reanalysis and the statistics are done from 90°E to 90°W.

vorticity ($f_0 + \varsigma_{gi}$) differs significantly in regions of cyclonic vorticity versus anticyclonic vorticity.

[5] Following *Pedlosky* [1987] and *Tan and Boyd* [2004], and integrating equation (1) vertically from the lower boundary to the upper boundary in each layer of the fluid with the corresponding vertical boundary conditions and the forcing/dissipation included leads to the following coupled quasigeostrophic potential vorticity equations(dimensionless)

$$\frac{\partial q_i}{\partial t} + J(\psi_i, q_i) = D_i + M_i - \nu\nabla^4\psi_i \tag{2}$$

along with zonally periodic boundary conditions and meridional boundary conditions

$$\frac{\partial \psi_i}{\partial x} = 0 \quad and \quad \frac{\partial^2 \bar{\psi}_i}{\partial t \partial y} = 0, \quad at \quad y = 0, L_y \tag{3}$$

where overbar is zonal-average operator. The quasi-geostrophic potential vorticity q_i is related to the stream function ψ_i through the relation:

$$q_i = \nabla^2\psi_i + (-1)^i F(\psi_1 - \psi_2) + \beta y \tag{4}$$

where $\beta = \beta_0 L^2/U$ is the nondimensional gradient of the Coriolis parameter, $F = f_0^2 L^2/[gD(\rho_2 - \rho_1)/\rho_2]$ is the internal Froude number, and $J(a, b) = \partial a/\partial x \bullet \partial b/\partial y - \partial a/\partial y \bullet \partial b/\partial x$ is the *Jacobian* operator.

[6] The first terms at the right hand side of equation (2), D_i, are the forcing and dissipation which take the form

$$D_i = (-1)^{i+1}\kappa_T\left[(\psi_1 - \psi_2) - \left(\psi_1^e - \psi_2^e\right)\right] - \left[(-1)^i + 1\right]\kappa_M\left(1 + \varepsilon\nabla^2\psi_i\right)\nabla^2\psi_i/2 \tag{5}$$

where $\varepsilon = \dfrac{U}{f_0 L}$ is the Rossby number, which is the radio of relative vorticity ς_{gi} to the planetary vorticity f_0. Equation (5) differ from their counterparts in the work of *Lee and Held* [1993] and *Esler and Haynes* [1999] by that the Ekman pumping here takes a nonlinear form and it has its origin from the divergence-vorticity term of the vorticity equation.

[7] The second terms at the right hand side of equation (2), M_i, are given by

$$M_i = (-1)^{i+1}\varepsilon F\nabla^2\psi_i\left[\frac{\partial}{\partial t}(\psi_1 - \psi_2) + J(\psi_i, \psi_1 - \psi_2)\right] \tag{6}$$

which are called the interface perturbation terms and due their existence to the motion of the interface of the fluids. M_i have their root in the divergence-vorticity term in the vorticity equation and was totally absent in the work of *Lee and Held* [1993] and *Esler and Haynes* [1999].

[8] The stream functions of the radiative equilibrium state ψ_1^e and ψ_2^e are chosen the same as *Esler and Haynes*' [1999] so that the shear flow has a parabolic jet profile in the upper level, i.e.,

$$U_1^e = -\partial\psi_1^e/\partial y = 4\left(1 - y/L_y\right)y/L_y$$
$$U_2^e = 0 \tag{7}$$

To solve numerically equation (2) with boundary conditions equation (3), we use the pseudospectral method for spatial discretization and the third-order Adams-Bashforth method for time-marching with the same basic functions as in the

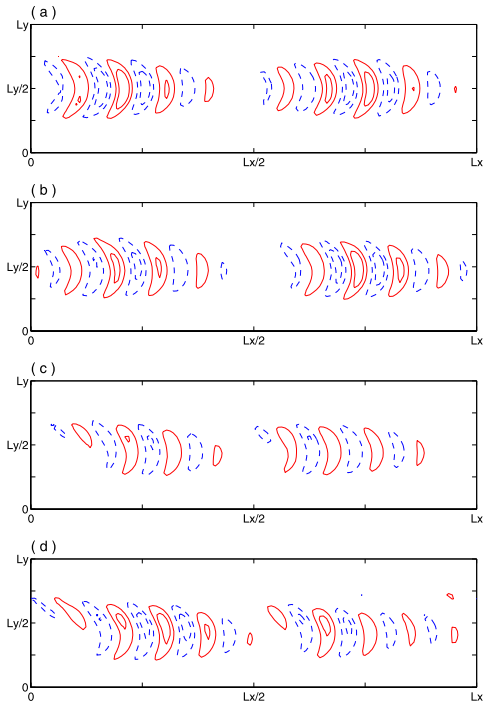

Figure 2. Snapshots of meridional velocity v′ of the upper layer: (a) $\varepsilon = 0$, (b) $\varepsilon = 0.1$, (c) $\varepsilon = 0.2$, and (d) $\varepsilon = 0.4$. Solid and dashed lines are positive and negative contours, respectively.

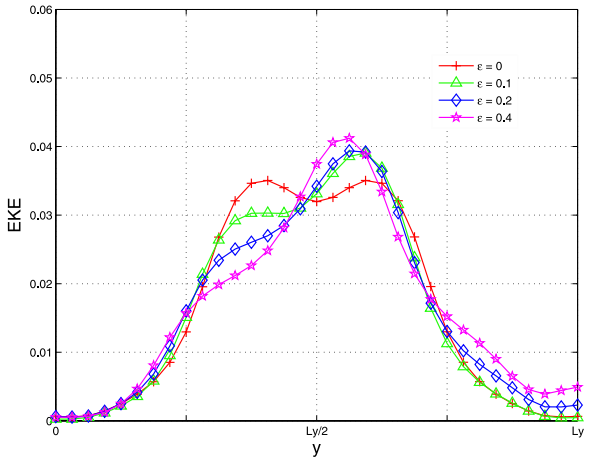

Figure 3. Meridional distribution of the time-and zonal-average eddy kinetic energy of the upper layer. Lines marked cross, triangle, diamond, and pentagram are the cases $\varepsilon = 0$, $\varepsilon = 0.1$, $\varepsilon = 0.2$, and $\varepsilon = 0.4$, respectively.

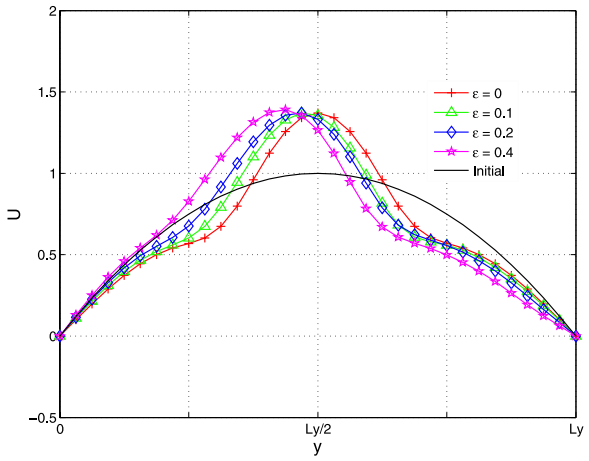

Figure 4. Meridional distribution of the time-and zonal-average flows of the upper layer. Lines marked cross, triangle, diamond, and pentagram are the time-average zonal flows for the cases $\varepsilon = 0$, $\varepsilon = 0.1$, $\varepsilon = 0.2$, and $\varepsilon = 0.4$, respectively. Solid black line is the initial radiative equilibrium flow.

work of *Boville* [1980]. The parameters are chosen as $L_x = 20\sqrt{2}\pi$, $Ly = 5\sqrt{2}\pi$, $F = 0.5$, $\beta = 0.25$, $k_M = 0.0354$, $\kappa_T = 0.0707$ and $\nu = 0.04$ while the Rossby number varies from case to case. In our numerical experiments 128 and 32 modes are used for x and y directions, respectively. As a check, we did some experiments with doubled spatial resolution but found no significant difference from the lower resolution reported here. Due to existence of the terms $\varepsilon F\nabla^2\psi_i\partial(\psi_2 - \psi_1)/\partial t$, one must invert a nonlinear operator to obtain an expression for the time derivatives at each time step. However, the nonlinear inversion can be actually be solved rapidly by using Newton's iteration because the Rossby number ε is small in our problem.

3. Numerical Results

[9] The numerical results are given in Figures 2–5. Figure 2 shows the snapshots of the meridional velocity of the upper layer. In Figure 2a $\varepsilon = 0$, which is the case in the work of *Lee and Held* [1993] and *Esler and Haynes* [1999]. Two wave packets are clearly seen and the structure asymmetry between the upstream and downstream sides of the wave packets is very significant, but there is no sign of north–south asymmetry for this case. Under the action of the nonlinear Ekman pumping and nonlinear interface perturbation, however, not only there exists asymmetry between the upstream and downstream parts of the wave packets, but a new asymmetry between the northern and southern parts upstream sets in. The northern of the wave packets upstream is stronger than its southern counterpart though the same asymmetry is not seen at the downstream part of the wave packets (Figures 2b, 2c, and 2d). Obviously the bigger the Rossby number is, the more significant the north–south asymmetry is.

[10] Naturally this north–south asymmetry is certainly reflected in the time-and zonal-average eddy kinetic energy associated with the baroclinic wave packets (Figure 3). When the Rossby number $\varepsilon = 0$, the wave packets are symmetry in north–south direction and there are two peaks in time-and-zonal-average across the channel. However, when the Rossby number differs from zero, the northern peak becomes stronger than the southern peak and this tendency is strengthened when the Rossby number becomes larger and finally southern peak gradually disappears and only northern peak is left.

[11] Figure 4 shows the meridional distribution of the time-average zonal flows for different Rossby numbers. Through complicated interaction between the eddies and the initial radiative equilibrium flow the initial zonal flow has been modified with its central part strengthened and the rest of the flow weakened. The time-average zonal flow still remains north–south symmetry for the case $\varepsilon = 0$. If the Rossby number differs from zero, however, the peak of the time-average zonal flows shifts southward, which leads to a

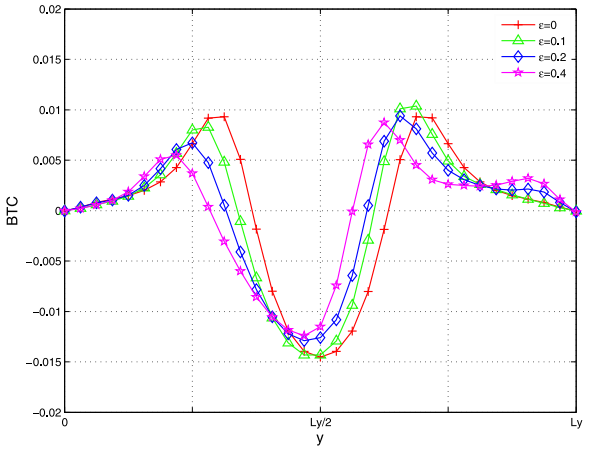

Figure 5. Barotropic energy conversion from the flow to the wave packets. Lines marked cross, triangle, diamond, and pentagram indicate the cases $\varepsilon = 0$, $\varepsilon = 0.1$, $\varepsilon = 0.2$, and $\varepsilon = 0.4$, respectively. Expression of the barotropic energy conversion term is the same as in the work of *Esler and Haynes* [1999].

latitude gap between the peaks of the time-and-zonal-average zonal flow and the eddy kinetic energy.

[12] Based on the same wave activity analysis by *Esler and Haynes* [1999], we know that both the barotropic and baroclinic energy conversions control the interaction between the zonal flow and the wave packets. However, it is the barotropic conversion that leads to the north–south asymmetry (Figure 5). At the central part of the channel, the barotropic conversion is negative, which means that the energy flows from the wave packets to the zonal flow while at the northern and southern parts of channel the energy conversion is from the zonal flow to the wave packets. If the Rossby number differs from zero, the barotropic conversion at the northern part is stronger than at the southern part, which causes the formation of the north–south asymmetry.

4. Discussion

[13] In this paper we have analyzed baroclinic wave packets in numerical experiments with a two-layer quasi-geostrophic model containing two kinds of nonlinearity. One kind of the nonlinearity is the advection of the potential vorticity, which has its origin in the advection of momentum in the primitive equations of motion. *Lee and Held* [1993], *Swanson and Pierrehumbert* [1994], and *Esler and Haynes* [1999] showed that it was this kind of nonlinearity that limited the upstream expansion of the wave packets and led to the downstream development of the baroclinic wave packets. Another kind of nonlinearity is the nonlinear Ekman pumping and nonlinear interface terms, which come from the divergence-vorticity term in the vorticity equation and also have their original root in the advection of the momentum in the primitive equations of motion. Our work here demonstrates that it is this kind of nonlinearity that leads to the north–south asymmetry of the storm track\ baroclinic wave packet dynamics. Indeed the nonlinear interface terms contribute dominantly to the formation of the north–south asymmetry and the effect of the Ekman pumping is very weak and negligible. This is because in our problem the order of the nonlinear interface terms is of $O(\varepsilon F)$ while the order of the nonlinear Ekman pumping is of $O(\varepsilon F \kappa_M)$ which is much smaller than the former for the Ekman friction parameter κ_M used in this paper is very small. As to the effects of the local change and advection terms in the nonlinear interface terms, they are of equal importance to the formation of the north–south asymmetry.

[14] The divergence-vorticity terms $(f_0 + \varsigma_{gi})\left(\frac{\partial u_i}{\partial x} + \frac{\partial v_i}{\partial y}\right)$ are of cyclone-anticyclone asymmetry, how do they result in the north–south asymmetry in structure of stormtracks? For a storm track associated with a strong east–west jet flow the divergence-vorticity terms are really assume a north–south asymmetry even for a jet which is initially a north–south symmetry. This is because that for an east–west jet flow the relative vorticity is cyclonic in its northern part and anticyclonic in its southern part. Based on such dominant background and through complicated nonlinear interactions between eddies and jet flow coupled with baroclinic instability, the finally equilibrated eddy-zonal flow system exhibits north–south asymmetry. Indeed experiments with other types of the initial jets, such as the Gaussian function as in the work of *Lee and Held* [1993], or the jet of north–south asymmetry show that the formation of the north–south asymmetry is not sensitive to the shape of the initial jets.

[15] No doubt that other factors such as the interactions between the subtropical and extratropical jets or between the subtropical jet and the Hedley cell [*Held and Hou*, 1980; *Kim and Lee*, 2004; *Walker and Schneider*, 2006], or the beta effect may be other possible factors that lead to the formation of the north–south asymmetry. Study on how the beta effect and the relative vorticity combined affect the storm track dynamics is now under its way.

[16] **Acknowledgments.** The authors are grateful for the suggestions from two anonymous reviewers. This work is supported by projects 40275012 and 40533016 supported by NSFC.

References

Berbery, E. H., and C. S. Vera (1996), Characteristics of the Southern Hemisphere winter storm track with filtered and unfiltered data, *J. Atmos. Sci.*, *53*, 468–481.

Boville, B. A. (1980), Amplitude vacillation on an f-plane, *J. Atmos. Sci.*, *37*, 1413–1423.

Chang, E. K. M. (1993), Downstream development of baroclinic waves as inferred from regression analysis, *J. Atmos.c Sci.*, *50*, 2038–2053.

Chang, E. K. M. (2001), The structure of baroclinic wave packets, *J. Atmos. Sci.*, *58*, 1694–1713.

Chang, E. K. M., and I. Orlanski (1993), On the dynamics of a storm track, *J. Atmos. Sci.*, *50*, 999–1015.

Chang, E. K. M., and D. B. Yu (1999), Characteristics of wave packets in the upper troposphere. Part I: Northern Hemisphere winter, *J. Atmos. Sci.*, *56*, 1708–1728.

Esler, J. G., and P. H. Haynes (1999), Mechanisms for wave packet formation and maintenance in a quasigeostrophic two-layer model, *J. Atmos. Sci.*, *56*, 2457–2490.

Held, I. M., and A. Y. Hou (1980), Nonlinear axially symmetric circulations in a nearly inviscid atmosphere, *J. Atmos. Sci.*, *37*, 515–533.

Kim, H. K., and S. Lee (2004), The wave-zonal flow interaction in the Southern Hemisphere, *J. Atmos. Sci.*, *61*, 1055–1067.

Lee, S., and I. M. Held (1993), Baroclinic wave packets in models and observations, *J. Atmos. Sci.*, *50*, 1413–1428.

Pedlosky, J. (1987), *Geophysical Fluid Dynamics*, 2nd ed., 710 pp., Springer, New York.

Simmons, A. J., and B. J. Hoskins (1979), Downstream and upstream development of unstable baroclinic waves, *J. Atmos. Sci.*, *36*, 1249–1254.

Swanson, K. L., and R. T. Pierrehumbert (1994), Nonlinear wave packets evolution on a baroclinically unstable jet, *J. Atmos. Sci.*, *51*, 384–394.

Tan, B. K., and J. P. Boyd (2004), Stable and unstable evolution of modons perturbed by surface term, bottom friction, and bottom topography incorporating nonlinear Ekman pumping, *J. Atmos. Sci.*, *61*, 310–323.

Walker, C. C., and T. Schneider (2006), Eddy influence on Hadley circulations: Simulations with an idealized GCM, *J. Atmos. Sci.*, *63*, 3333–3350.

P. Lin, J. Nie, B. Tan, and W. Yang, Laboratory of Severe Storm and Flood Disaster, Department of Atmospheric Sciences, School of Physics, Peking University, Beijing 100871, China. (bktan@pku.edu.cn)